

Supplementary Materials for

Biogeochemical controls of surface ocean phosphate

Adam C. Martiny*, Michael W. Lomas, Weiwei Fu, Philip W. Boyd, Yuh-ling L. Chen, Gregory A. Cutter, Michael J. Ellwood, Ken Furuya, Fuminori Hashihama, Jota Kanda, David M. Karl, Taketoshi Kodama, Qian P. Li, Jian Ma, Thierry Moutin, E. Malcolm S. Woodward, J. Keith Moore

*Corresponding author. Email: amartiny@uci.edu

Published 28 August 2019, *Sci. Adv.* **5**, eaax0341 (2019)

DOI: 10.1126/sciadv.aax0341

This PDF file includes:

Fig. S1. Systematic bias in predicted phosphate concentrations.

Fig. S2. Relationship between observed DIP ($[DIP]_{obs}$) and shipboard NPP (NPP_{obs}).

Fig. S3. Relationship between predicted surface DIP ($[DIP]_{predict}$) and predicted chlorophyll concentrations ($Chl_{predict}$) across ESMs.

Fig. S4. Relationship between predicted surface DIP ($[DIP]_{predict}$) and predicted integrated NPP ($NPP_{predict}$) across ESMs.

Fig. S5. Comparison of the predicted surface DIP distribution between CESM1 and CESM2.

Fig. S6. Distribution and changes to the predicted atmospheric Fe deposition and N fixation in the global ocean.

Fig. S7. Predicted global variation in the vertical velocity.

Fig. S8. Relationship between the vertical velocity and observed near-surface DIP concentrations.

Fig. S9. Elemental supply ratios in nutricline waters.

Table S1. ESMs used in this study.

Table S2. Abbreviations.

References (57–62)

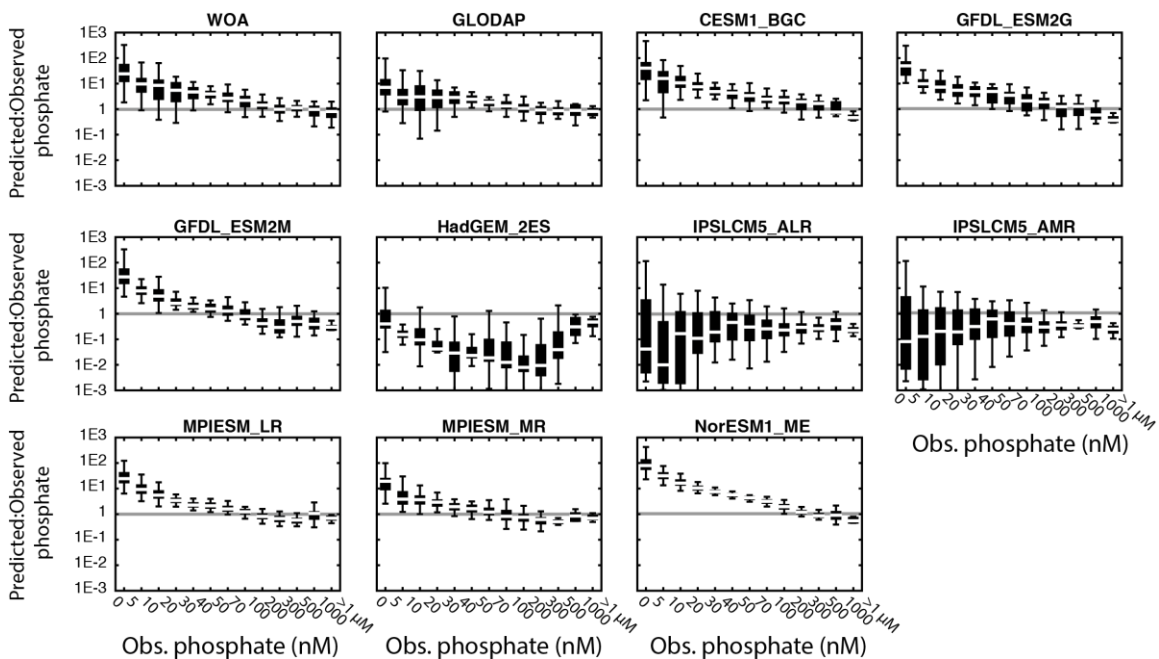


Fig. S1. Systematic bias in predicted phosphate concentrations. $[DIP]_{obs}$ ($n = 1138$) are median concentrations in $1^\circ \times 1^\circ$ grids from the top 30 m and then binned by level. Each is matched to a predicted value ($[DIP]_{predict}$) for the same location. Model predictions are from the CMIP5 model comparison project. Box plots are drawn with default levels (white line = median, boxes cover 25 to 75%, and whiskers cover 2.5 to 97.5%).

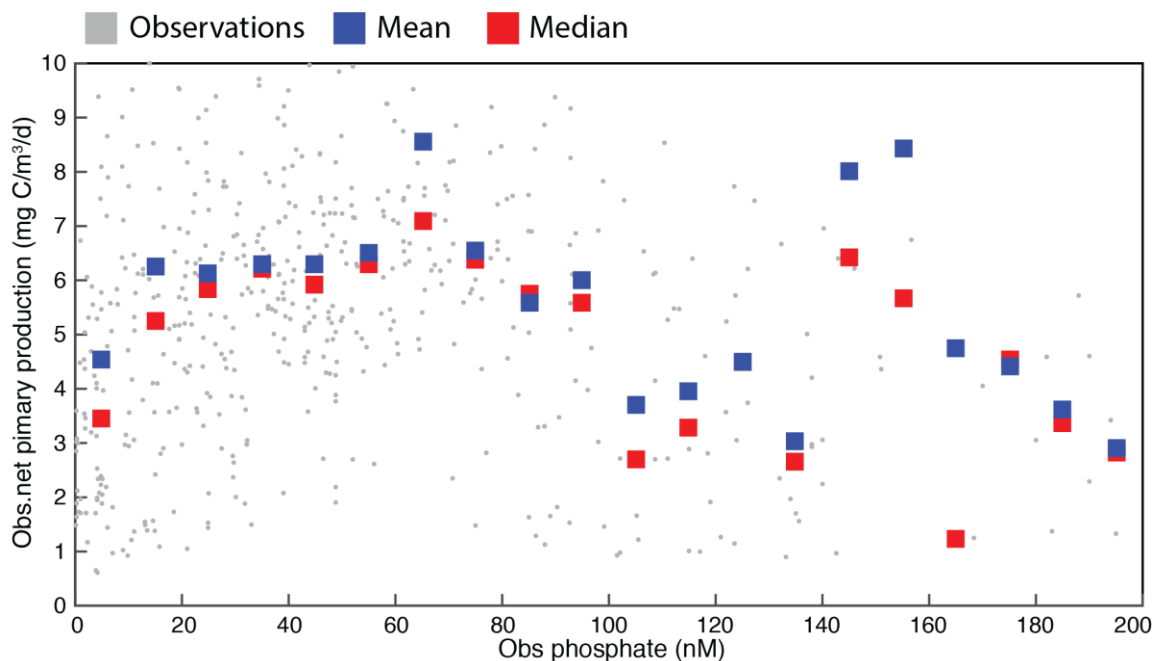


Fig. S2. Relationship between observed DIP ($[DIP]_{obs}$) and shipboard NPP (NPP_{obs}).

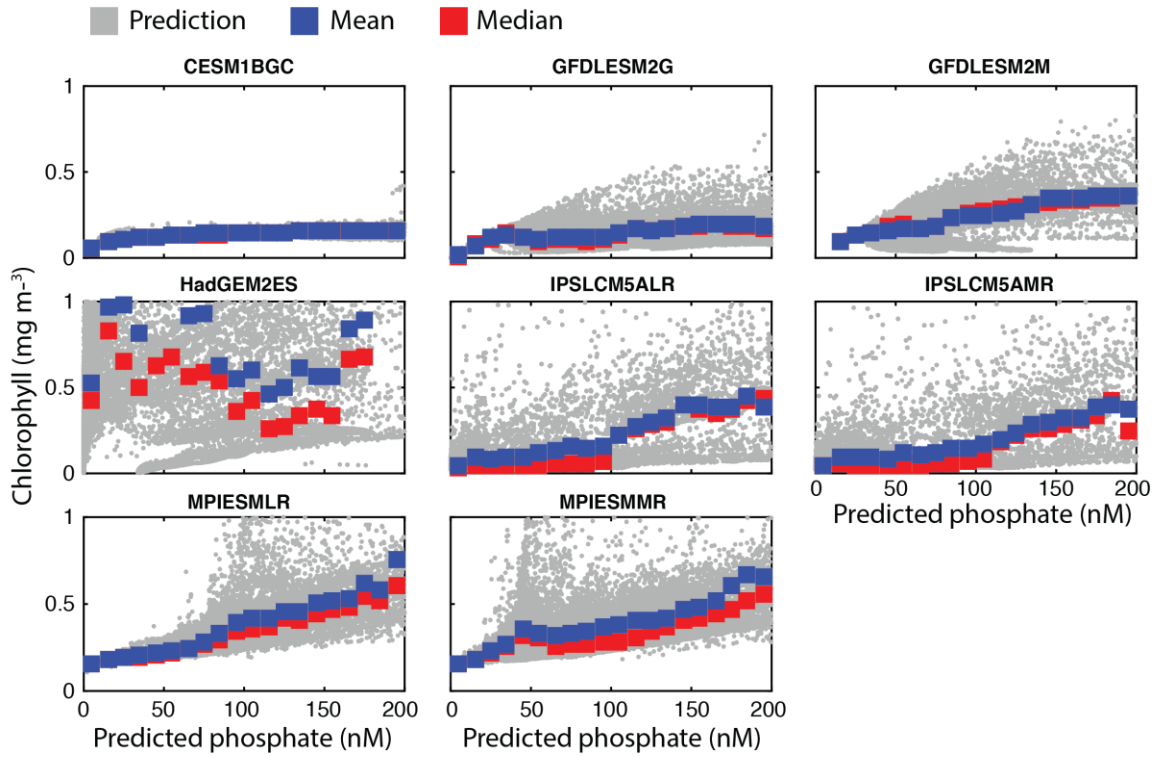


Fig. S3. Relationship between predicted surface DIP ($[DIP]_{\text{predict}}$) and predicted chlorophyll concentrations (Chl_{predict}) across ESMs. Model predictions are from the CMIP5 model comparison project.

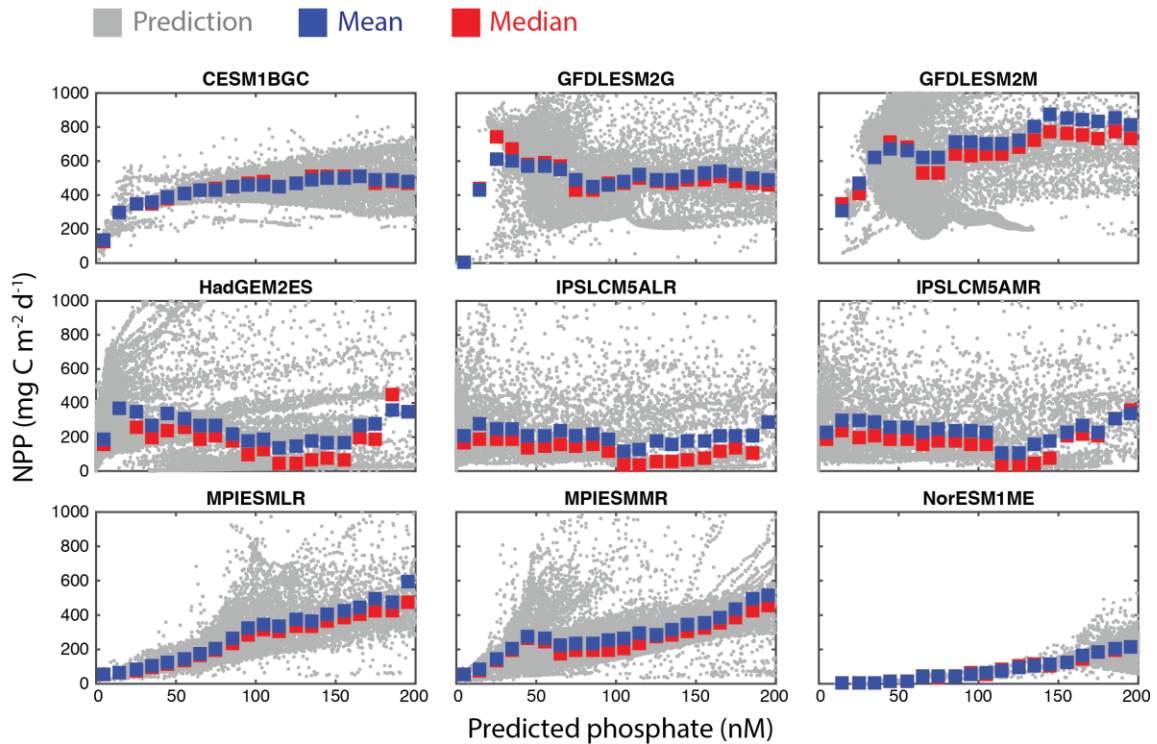


Fig. S4. Relationship between predicted surface DIP ($[DIP]_{\text{predict}}$) and predicted integrated NPP (NPP_{predict}) across ESMs. Model predictions are from the CMIP5 model comparison project.

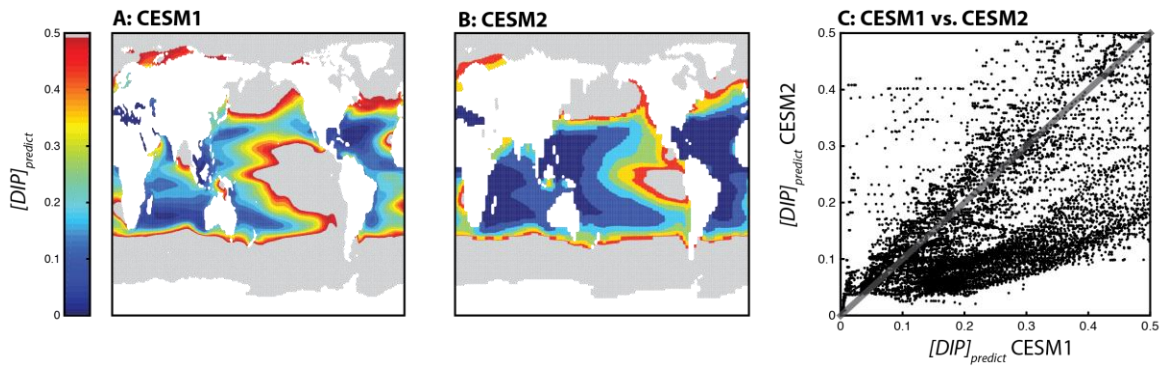


Fig. S5. Comparison of the predicted surface DIP distribution between CESM1 and CESM2. A: The geospatial pattern of surface $[DIP]_{predict}$ in CESM1 and **B:** CESM2. **C:** A direct comparison between predicted DIP for each model.

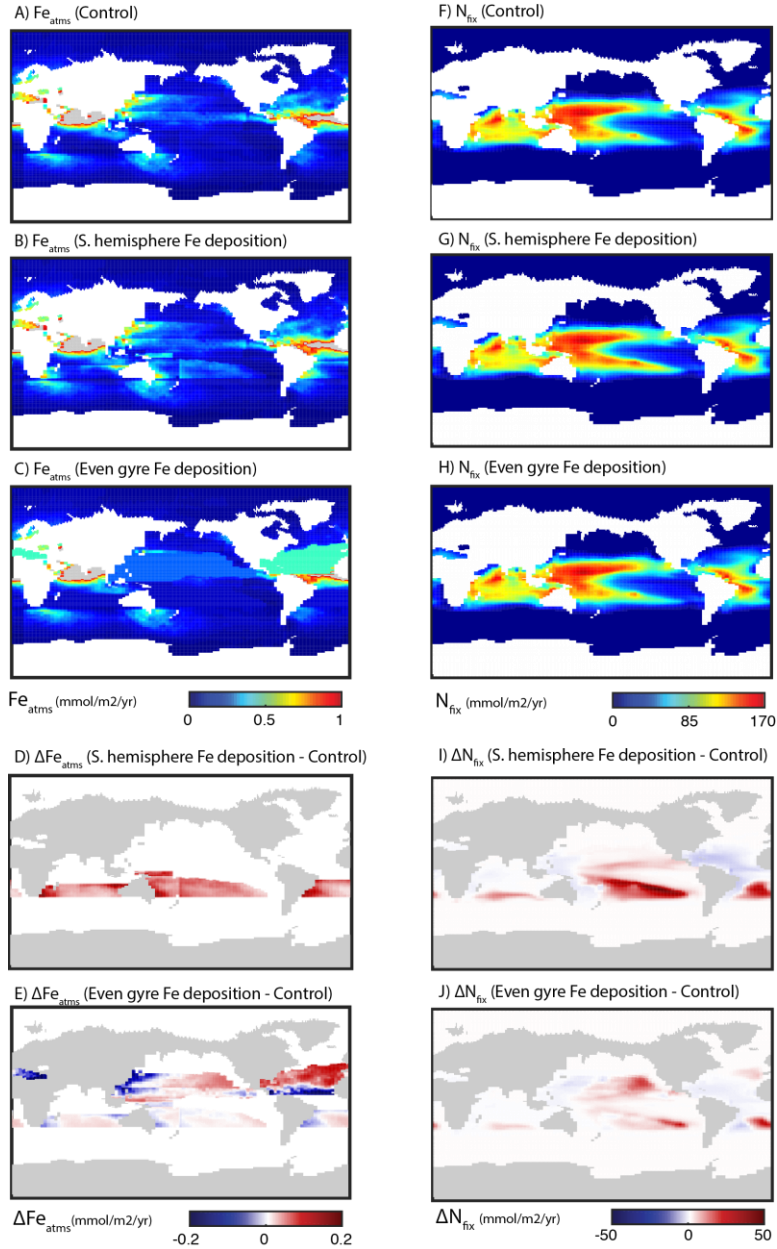


Fig. S6. Distribution and changes to the predicted atmospheric Fe deposition and N fixation in the global ocean. **A:** Estimated Fe deposition (Fe_{atms}) in the current ocean (i.e., control scenario). **B:** Fe deposition for the scenario of increased dust deposition in the southern hemisphere gyres (reaching N. Pacific Ocean Subtropical Gyre levels). **C:** Fe deposition for the scenario of even dust deposition within each subtropical gyre. **D:** Differences in Fe deposition between southern hemisphere scenario (as shown in B) and current levels (as shown in A). **E:** Differences in dust deposition between 'even gyre scenario' (as shown in C) and current levels (as shown in A). **F:** Nitrogen fixation (N_{fix}) based on current Fe deposition levels. **G:** Nitrogen fixation based on increased Fe deposition in the southern hemisphere gyres. **H:** Nitrogen fixation based on even dust deposition across each subtropical gyre. **I:** Differences in nitrogen fixation between a scenario with increased Fe deposition in southern hemisphere Fe deposition (as shown in G) vs. current levels (shown in F). **J:** Differences in nitrogen fixation between a scenario with even Fe deposition in each gyre (as shown in H) vs. current levels (shown in F). The Fe deposition and N fixation rates are simulated in CESM v2.

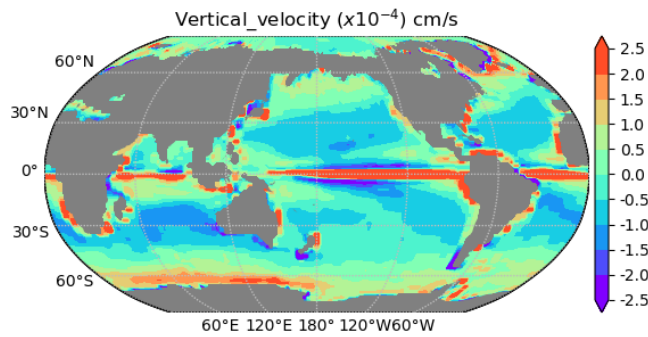


Fig. S7. Predicted global variation in the vertical velocity. Positive vertical velocity values indicate upwelling and negative equals downwelling,

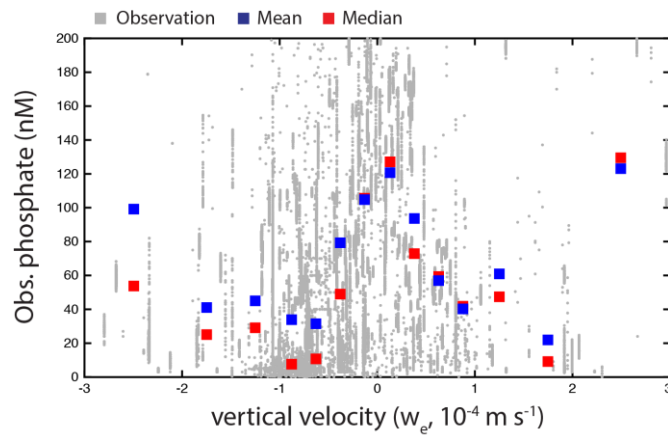


Fig. S8. Relationship between the vertical velocity and observed near-surface DIP concentrations. Positive vertical velocity values indicate upwelling and negative equals downwelling,

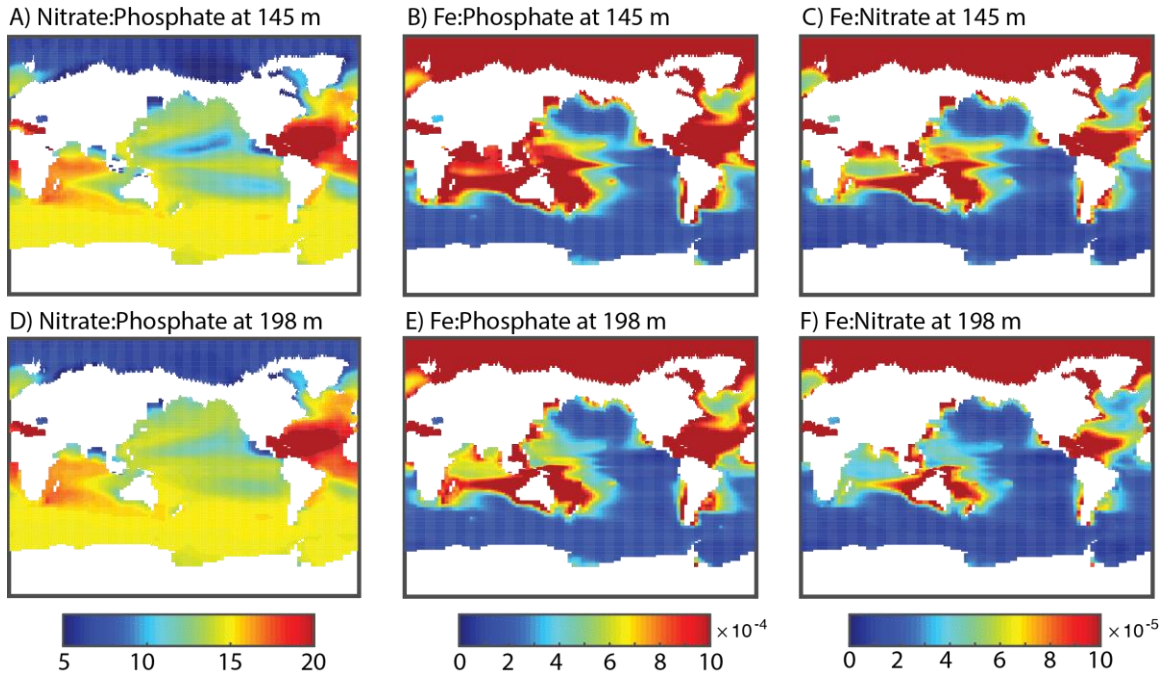


Fig. S9. Elemental supply ratios in nutricline waters. (A-C) Supply ratios at 145 m depth. (D-F) Supply ratios at 198 m depth. 145 m and 198 m corresponded to the two depth levels in CESM at the bottom of euphotic zone and were chosen as representatives of nutrient levels/ratios of nutricline water being vertically supplied to the surface ocean. The supply ratios are from the control simulation in CESM v2.

Table S1. ESMs used in this study.

ESM Model	Ocean module	Depth layers	Chl	NPP	Resolution	Reference
CESM1-BGC	BEC	60	X	X	1.125°/0.27°-0.53°	(57)
GFDL-ESM2G	TOPAZ2	63	X	X	0.3–1°	(58)
GFDL-ESM2M	TOPAZ2	50	X	X	0.3–1°	(58)
HadGEM2-ES	Diat-HadOCC	40	X	X	0.3–1°	(59)
IPSL-CM5A-LR	PISCES	31	X	X	0.5–2°	(60)
IPSL-CM5A-MR	PISCES	31	X	X	0.5–2°	(60)
MPI-ESM-LR	HAMOCC5.2	40	X	X	1.5°	(61)
MPI-ESM-MR	HAMOCC5.2	40	X	X	0.4°	(61)
NorESM1-ME	HAMOCC5.1	53		X	1.125°	(62)

Table S2. Abbreviations.

Variable	Description	Unit
<i>[DIP]_{obs}</i>	Observed phosphate using high sensitivity techniques	nM
<i>[DIP]_{predict}</i>	Phosphate predicted by climatologies and ESMs	nM
<i>Chl_{sat}</i>	Chlorophyll concentrations estimated by satellite	mg m ⁻³
<i>Chl_{predict}</i>	Chlorophyll concentrations predicted by ESMs	mg m ⁻³
<i>NPP_{obs}</i>	Net primary production observed	mg C m ⁻³ d ⁻¹
<i>NPP_{sat}</i>	Integrated net primary production estimated by satellite	mg C m ⁻² d ⁻¹
<i>NPP_{predict}</i>	Integrated net primary production predicted by ESMs	mg C m ⁻² d ⁻¹
<i>Fe_{atms}</i>	Atmospheric deposition of dissolved iron	mmol Fe m ⁻² yr ⁻¹